

# Polymer species in aqueous solutions of *para*-phenylenediamine-*N,N,N',N'*-tetraacetic acid (*p*-PhDTA) with cobalt(II), nickel(II), copper(II), zinc(II) and cadmium(II). X-ray crystal structure of $\text{Na}_4[\text{Co}_2(\textit{p}\text{-PhDTA})_2] \cdot 8\text{H}_2\text{O}$

Carlos A. González,<sup>a</sup> Margarita Hernández-Padilla,<sup>a</sup> Sixto Domínguez,<sup>a</sup> Alfredo Mederos,<sup>a\*</sup> Felipe Brito<sup>b</sup> and Juan M. Arrieta<sup>c</sup>

<sup>a</sup> Departamento de Química Inorgánica, Universidad de La Laguna, Tenerife, Canary Islands, Spain

<sup>b</sup> Laboratorio de Equilibrios en Solución, Escuela de Química, Facultad de Ciencias, Universidad Central de Venezuela, Caracas, Venezuela

<sup>c</sup> Departamento de Química Inorgánica, Universidad del País Vasco, Apartado 644, Bilbao, Spain

(Received 2 July 1996; accepted 31 January 1997)

**Abstract**—Potentiometric investigations in aqueous solutions at 25°C and ionic strength 0.1 ( $\text{Cu}^{\text{II}}$ ,  $\text{Ni}^{\text{II}}$ ,  $\text{Co}^{\text{II}}$ ,  $\text{Zn}^{\text{II}}$  and  $\text{Cd}^{\text{II}}$ ) and 0.5 mol dm<sup>-3</sup> KCl ( $\text{Cu}^{\text{II}}$ ) analysed by LETAGROP and simulation calculus for a three-component system [Z(pH) curves] show that *p*-phenylenediamine-*N,N,N',N'*-tetraacetic acid (*p*-PhDTA) forms protonated and non-protonated monomer and polymer complexes (ligand,  $\text{H}_4\text{L}$ ) at the concentrations and ligand: metal ratio studied: ratio 1:1, complexes  $\text{H}_i\text{M}_n\text{L}_n^{(2n-i)-}$ ,  $n = 1-3, 5, 6$  ( $\text{Cu}^{\text{II}}$ ,  $\text{Ni}^{\text{II}}$  and  $\text{Co}^{\text{II}}$ ) and  $n = 1-3$  ( $\text{Zn}^{\text{II}}$  and  $\text{Cd}^{\text{II}}$ ); with excess of metal complexes  $\text{H}_i\text{M}_{n+1}\text{L}_n^{(2n-2-i)-}$ ,  $n = 1$  for all cations and  $n = 2, 3$  for  $\text{Ni}^{\text{II}}$  and  $\text{Co}^{\text{II}}$ ; with excess of ligand, complexes  $\text{H}_i\text{M}_n\text{L}_{n+1}^{(2n+4-i)-}$ , with  $n = 1$  mainly. The formation constants  $\beta_{pq}$  of the complexes have been determined and the Irving-Williams order of complexation is fulfilled. The species distribution diagrams indicate that the more important non-protonated polymer complexes are: trimer and pentamer for  $\text{Cu}^{\text{II}}$ ; pentamer for  $\text{Ni}^{\text{II}}$ ; dimer and trimer for  $\text{Co}^{\text{II}}$ ; trimer for  $\text{Zn}^{\text{II}}$  and  $\text{Cd}^{\text{II}}$ .  $\text{Co}^{\text{II}}$ ,  $\text{Ni}^{\text{II}}$  and  $\text{Cu}^{\text{II}}$  also form hexamers. From a concentrated solution with a ligand: metal ratio 2:3 at pH 5, single crystals of the complex  $\text{Na}_4[\text{Co}_2(\textit{p}\text{-PhDTA})_2] \cdot 8\text{H}_2\text{O}$  were obtained. X-ray diffraction structural analysis revealed that in the dimer anion  $[\text{Co}_2(\textit{p}\text{-PhDTA})_2]^{4-}$  the cobalt atoms are hexa-coordinated with each metal surrounded by four carboxylic oxygens and two amine nitrogens (from two iminodiacetate groups) in a distorted octahedron. Each sodium is coordinated to water molecules and carboxyl groups, being five-coordinated. © 1997 Elsevier Science Ltd

**Keywords:** *para*-phenylene-tetraacetate; polymer complexes; stability constants; cobalt(II), nickel(II); copper(II).

Diaminetetramethylenecarboxylic acids derived from *m*- or *p*-phenylenediamines can only coordinate one nitrogen atom to any one metal cation. These ligands can therefore coordinate in two spheres, as has been proven by the preparation of bimetallic species  $\text{M}_2\text{L}$  (ligands,  $\text{H}_4\text{L}$ ) in the solid state [1–2] and in studies

in aqueous solution [3–6] for *m*-PhDTA (*meta*-phenylenediamine-*N,N,N',N'*-tetraacetic acid) and *p*-PhDTA (*para*-phenylenediamine-*N,N,N',N'*-tetraacetic acid). The formation of species with excess of ligand is also possible since each iminodiacetic group of the ligand is insufficient coordinatively to saturate the central ion, as confirmed by our studies in aqueous solution of the coordinating ability of *m*-PhDTA and *p*-PhDTA with  $\text{Cu}^{\text{II}}$  [6].

\* Author to whom correspondence should be addressed.

In the case of ligands derived from *m*-phenylenediamines, the special conformation of the ligand with nitrogen atoms in *meta* positions on the aromatic ring facilitates the formation of dimer complexes since the ligands act as a bridge. This has been proven in the case of *m*-PhDTA acid by means of studies in aqueous solution with  $\text{Co}^{\text{II}}$  [7],  $\text{Ni}^{\text{II}}$  [8] and  $\text{Cu}^{\text{II}}$  [9]. After studying the conditions for the formation of the dimer species  $\text{M}_2\text{L}_2^{4-}$  in aqueous solution, a single crystal of each of the complexes  $\text{Na}_4[\text{Cu}_2(\text{m-PhDTA})_2] \cdot 18\text{H}_2\text{O}$  and  $\text{Na}_4[\text{Co}_2(\text{m-PhDTA})_2] \cdot 10\text{H}_2\text{O}$ , respectively, were obtained and their structures were determined by X-ray diffraction analysis [9]. Similar studies with 2,6-TDTA [10] and 2,4-TDTA [11] acids have been performed.

Consequently, it is to be expected that the *para* positions of the nitrogen atoms on the aromatic rings in *p*-PhDTA acid facilitates the formation of polymer complexes since the ligand acid acts as a bridge: with divalent cations in the 1:1 ratio, the ligand can form  $\text{ML}_2^{2-}$  monomer complexes or  $\text{M}_n\text{L}_n^{2n-}$  polymer complexes; with excess of metal it can form  $\text{M}_2\text{L}$  bimetallic species or  $\text{M}_{n+1}\text{L}_n^{2(n-1)-}$  polymer species; and with excess of ligand it can form  $\text{ML}_2^{6-}$  monomer species or  $\text{M}_n\text{L}_{n+1}^{(2n+4)-}$  polymer species. All these different types of complexes can be protonated and thus can give rise to a wide variety of complexes.

In this work, a study of the conditions for the formation in aqueous solution of polymer species  $\text{M}_n\text{L}_n^{2n-}$ ,  $\text{M}_{n+1}\text{L}_n^{2(n-1)-}$  and  $\text{M}_n\text{L}_{n+1}^{(2n+4)-}$  has been carried out for *p*-PhDTA with  $\text{Co}^{\text{II}}$ ,  $\text{Ni}^{\text{II}}$ ,  $\text{Cu}^{\text{II}}$ ,  $\text{Zn}^{\text{II}}$  and  $\text{Cd}^{\text{II}}$ , using different ligand: metal ratios, *R*. Previous studies of these systems [4–6] did not take into account the possible presence of these species.

## EXPERIMENTAL

### Preparation of $\text{NaH}_3(\text{p-PhDTA}) \cdot \text{H}_2\text{O}$

The monosodic salt of *p*-PhDTA was prepared in a similar manner to the Blasius and Olbrich method for *m*-PhDTA acid [12], with some modifications: ratio chloroacetic acid: *p*-phenylenediamine dihydrochloride 6:1; 70–80°C, pH > 10; after the reaction was completed, HCl (25%) was added to pH 3, to afford a white precipitate of the monosodic salt of *p*-PhDTA acid.

The product was filtered and washed with cold water and acetone and dried to  $T < 50^\circ\text{C}$  until constant weight. Found: C, 44.8; H, 3.9; N, 7.6; Na, 6.0. Calc. for  $\text{C}_{14}\text{H}_{15}\text{N}_2\text{O}_8\text{Na} \cdot \text{H}_2\text{O}$ : C, 44.2; H, 4.5; N, 7.4; Na 6.0%. Elemental analyses were performed on a Carlo-Erba 1106 automatic analyser. Sodium was determined by atomic absorption on a Pye Unicam SP 1900. Precautions were taken to maintain an inert atmosphere (argon) and prevent the access of light during the preparation and preservation of the ligand and during the study of its solutions, since it is photosensitive and oxidizes readily.

### EMF measurements

The potentiometric titrations were carried out in aqueous solution at 25°C and 0.1 mol dm<sup>-3</sup> KCl ( $\text{Co}^{\text{II}}$ ,  $\text{Ni}^{\text{II}}$ ,  $\text{Cu}^{\text{II}}$ ,  $\text{Zn}^{\text{II}}$  and  $\text{Cd}^{\text{II}}$ ) and 0.5 mol dm<sup>-3</sup> KCl ( $\text{Cu}^{\text{II}}$ ). The sealed 100 cm<sup>3</sup> thermostated double-walled glass reaction vessel was fitted with a Radiometer G202B glass electrode, a Radiometer K711 calomel reference electrode, inert argon atmosphere inlet and outlet tubes, a magnetic stirrer and a titrant inlet. Readings of potentials were obtained with a Radiometer type PHM-85 potentiometer. The titrant was delivered through an immersed capillary tip from a Crisson Microbur 2031 piston buret and the temperature was maintained at  $25.00 \pm 0.01^\circ\text{C}$  by circulation of water from a refrigerated constant-temperature bath. A basic program [13] (APT program from micro-computer ITS80286) was used to monitor, for each titration point, the emf values and the volume of titrant added. When the observed emf was constant, within user-defined limits, the next volume of titrant was added automatically and the cycle repeated until predefined total volume of titrant had been added. The cell constants  $E^\circ$  and the liquid junction potential constant  $J$  of the equation  $E = E^\circ + J[\text{H}^+] + 59.16 \log [\text{H}^+]$  were determined according to Biedermann and Sillén [14] and the data analysed using the program NERNST/LETA [15], a version of the least-squares program LETAGROP [16]. A carbonate-free sodium hydroxide solution was prepared according to ref. [17] and standardized against potassium hydrogenphthalate. The metal solutions were standardized potentiometrically against  $\text{Na}_2\text{EDTA}$  and the data analyzed by means of the program NERNST/LETA [18]. The reagents HCl, NaOH, KCl,  $\text{CoCl}_2$ ,  $\text{NiCl}_2$ ,  $\text{CuCl}_2$ ,  $\text{ZnCl}_2$  and  $\text{CdCl}_2$  were Merck p.a. The KCl was recrystallized once. The compounds chloroacetic acid and *p*-phenylenediamine dihydrochloride were Merck for synthesis and Fluka puriss., respectively.

Measurements were taken of the ligand alone (Table 1) and the ligand in the presence of metallic cation (titrations with NaOH); Table 2 for  $\text{Cu}^{\text{II}}$  ( $I = 0.5$  and  $0.1 \text{ mol dm}^{-3}$ ) and Table 3 for  $\text{Ni}^{\text{II}}$ ,  $\text{Co}^{\text{II}}$ ,  $\text{Zn}^{\text{II}}$  and  $\text{Cd}^{\text{II}}$  ( $I = 0.1 \text{ mol dm}^{-3}$ ).

The search for the presence of the polymer complexes was carried out by titrations at different concentrations, ratio of ligand: metal was 1:1 mainly, and also with an excess of ligand (to search complexes with excess of ligand) and an excess of metal (to search complexes with excess of metal).

The experimental data were analysed by means of NERNST/LETA [15]. It was found that under the experimental conditions used, hydrolysis of the metallic cations was negligible. For the ligand at  $I = 0.1 \text{ mol dm}^{-3}$ , the SUPERQUAD program was also used [19], with identical results.

$\text{Cu}^{\text{II}}$  experiments were carried out in KCl 0.1 and 0.5 mol dm<sup>-3</sup> as inert ionic media [14,20], in order to verify the stability of the polymer species upon variation of the ionic medium.

Table 1. Ionization constants of the *p*-PhDTA acid (25°C; *I* = 0.5 and 0.1 mol dm<sup>-3</sup> in KCl)

Equilibrium	<i>pr</i>	<i>I</i> = 0.5 <sup>a</sup>		<i>I</i> = 0.1 <sup>b</sup>		2,5-TDTA		
		log β <sub><i>pr</i></sub>	p <i>K</i> <sub>i</sub>	log β <sub><i>pr</i></sub>	p <i>K</i> <sub>i</sub>			
(4) HL <sup>3-</sup> /L <sup>4-</sup>	11	5.652 ± 0.018	5.65	6.045 ± 0.008	6.05	6.04 <sup>c</sup>	6.11 <sup>c</sup>	7.21 <sup>c</sup>
(5) H <sub>2</sub> L <sup>2-</sup> /HL <sup>3-</sup>	21	10.258 ± 0.016	4.61	10.893 ± 0.005	4.85	4.91	4.87	4.55
(6) H <sub>3</sub> L <sup>-</sup> /H <sub>2</sub> L <sup>2-</sup>	31	13.017 ± 0.030	2.76	13.788 ± 0.008	2.90	2.90	2.87	2.44
(7) H <sub>4</sub> L/H <sub>3</sub> L <sup>-</sup>	41	15.113 ± 0.059	2.09	15.884 ± 0.012	2.10	2.00	1.83	1.85
(8) H <sub>5</sub> L <sup>+</sup> /H <sub>4</sub> L	51	17.469 ± 0.033	2.36	17.636 ± 0.016	1.75			1.97

<sup>a</sup> Three titrations (*C*<sub>L</sub> = 0.523 × 10<sup>-3</sup> and 1.027 × 10<sup>-3</sup> mol dm<sup>-3</sup>, titrations with NaOH; *C*<sub>L</sub> = 1.012 × 10<sup>-3</sup> mol dm<sup>-3</sup> titration with HCl); 124 points; LETAGROP, σ(*Z*) = 0.015; -log[H<sup>+</sup>] range, 2.13–6.17.

<sup>b</sup> Four (*C*<sub>L</sub> = 1.95 × 10<sup>-3</sup>, 1.86 × 10<sup>-3</sup> and 1.97 × 10<sup>-3</sup> mol dm<sup>-3</sup>, titrations with NaOH; *C*<sub>L</sub> = 2.05 × 10<sup>-3</sup> mol dm<sup>-3</sup> titrations with HCl); 180 points; LETAGROP, σ(*Z*) = 0.018; SUPERQUAD, σ(*E*) = 0.196; chi<sup>2</sup> = 17.60; -log[H<sup>+</sup>] range 2.00–8.91.

<sup>c</sup> Ref. [34].

<sup>d</sup> Ref. [6].

<sup>e</sup> Ref. [28].

Table 2. Formation constants (log β<sub>*pqr*</sub>) for *p*-PhDTA acid with Cu<sup>II</sup> (25°C; *I* = 0.5 and 0.1 mol dm<sup>-3</sup>; ligand H<sub>4</sub>L)

<i>pqr</i>	Species	<i>I</i> = 0.5 <sup>a</sup>	<i>I</i> = 0.1 <sup>b</sup>
211	[H <sub>2</sub> ML]	15.41 ± 0.02	15.42 ± 0.02
111	[HML] <sup>-</sup>	12.78 ± 0.02	12.85 ± 0.02
011	[ML] <sup>2-</sup>	Max. 7.53	Max. 7.44
222	[H <sub>2</sub> M <sub>2</sub> L <sub>2</sub> ] <sup>2-</sup>	27.29 ± 0.10	27.41 ± 0.07
122	[HM <sub>2</sub> L <sub>2</sub> ] <sup>3-</sup>	23.65 ± 0.12	Max. 23.27
022	[M <sub>2</sub> L <sub>2</sub> ] <sup>4-</sup>	Max. 18.80	Max. 18.68
133	[HM <sub>3</sub> L <sub>3</sub> ] <sup>5-</sup>	35.32 ± 0.07	35.36 ± 0.05
033	[M <sub>3</sub> L <sub>3</sub> ] <sup>6-</sup>	30.89 ± 0.06	Max. 30.34
044	[M <sub>4</sub> L <sub>4</sub> ] <sup>8-</sup>	—	—
055	[M <sub>5</sub> L <sub>5</sub> ] <sup>10-</sup>	53.01 ± 0.19	53.02 ± 0.09
066	[M <sub>6</sub> L <sub>6</sub> ] <sup>12-</sup>	Max. 64.34	Max. 63.58
121	[HM <sub>2</sub> L] <sup>+</sup>	14.93 ± 0.15	Max. 14.88
021	[M <sub>2</sub> L]	12.42 ± 0.02	12.84 ± 0.08
032	[M <sub>3</sub> L <sub>2</sub> ] <sup>2-</sup>	—	—
412	[H <sub>4</sub> ML <sub>2</sub> ] <sup>2-</sup>	29.62 ± 0.10	—
312	[H <sub>3</sub> ML <sub>2</sub> ] <sup>3-</sup>	26.33 ± 0.08	—
212	[H <sub>2</sub> ML <sub>2</sub> ] <sup>4-</sup>	22.22 ± 0.07	—
112	[HML <sub>2</sub> ] <sup>5-</sup>	16.82 ± 0.12	—
012	[ML <sub>2</sub> ] <sup>6-</sup>	—	—
223	[H <sub>2</sub> M <sub>2</sub> L <sub>3</sub> ] <sup>6-</sup>	Max. 33.67	—

<sup>a</sup> No. of titrations 5 (ratio 1:1, *C*<sub>M</sub> = 1, 2 and 16 × 10<sup>-3</sup> mol dm<sup>-3</sup>; L:M 4:1 and 1:4, *C*<sub>M</sub> = 4 × 10<sup>-3</sup> mol dm<sup>-3</sup>); No. points 152; [σ(*Z*)] = 0.015; -log[H<sup>+</sup>] range, 2.56–5.77.

<sup>b</sup> No. of titrations 6 (ratio 1:1, *C*<sub>M</sub> = 2, 6, 15, 20 and 30 × 10<sup>-3</sup> mol dm<sup>-3</sup>; L:M 1:3; *C*<sub>M</sub> = 2 × 10<sup>-3</sup> mol dm<sup>-3</sup>); No. points 345; [σ(*Z*) = 0.032; -log[H<sup>+</sup>] range 2.12–5.42.

Experiments could not be performed for Zn<sup>II</sup> and Cd<sup>II</sup> at higher concentrations than *C*<sub>M</sub> > 1 × 10<sup>-3</sup> mol dm<sup>-3</sup>, because the corresponding complexes caused precipitation [4].

However, experiments were carried out, especially for *R* = 1/1, up to concentrations of *C*<sub>M</sub> = 30 × 10<sup>-3</sup> mol dm<sup>-3</sup> for Co<sup>II</sup> and Cu<sup>II</sup> and to 50 × 10<sup>-3</sup> mol dm<sup>-3</sup> in the case of Ni<sup>II</sup>.

Since these high concentrations may exceed the limits established in the inert ionic medium method [14,20], the data were analysed as follows:

In a first series, the curves were analysed in the ratio 1:1 to a maximum of *C*<sub>M</sub> = 15 × 10<sup>-3</sup> mol dm<sup>-3</sup>. Subsequently, the curves with *C*<sub>M</sub> > 15 × 10<sup>-3</sup> mol dm<sup>-3</sup> were analysed in another series. The calculations proved that the stability constants of the species formed were practically identical.

In the ionic medium KCl 0.5 mol dm<sup>-3</sup>, the 1:1 data were processed in a single series, because the concentration of reagents and products was always maintained below 20% of the concentration of the ions in the medium [14,20].

Spectrophotometric studies in aqueous solution are not possible by the very weak intensity of the field ligand bands of the Co<sup>II</sup>, Ni<sup>II</sup> and Cu<sup>II</sup> complexes and time dependence of the coloured band of the ligand [21,22].

#### Preparation of the complex Na<sub>4</sub>[Co<sub>2</sub>(*p*-PhDTA)<sub>2</sub>] · 8H<sub>2</sub>O

A concentrated aqueous solution of Na(*p*-PhDTA) · H<sub>2</sub>O (2 g) was mixed in the ratio ligand:metal 2:3 (to avoid the formation of complex species with the excess of ligand) with a concentrated solution of Co(NO<sub>3</sub>)<sub>2</sub> · 6H<sub>2</sub>O. By addition of NaOH solution the pH was fixed at 5 [predominance of the polymer species Co<sub>n</sub>L<sub>n</sub><sup>2n-</sup>, see species distribution diagram, Fig. 8(b)]. Addition of ethanol to the solution resulted in the precipitation of a pinkish violet polycrystalline dust. The precipitate was filtered off, washed several times with ethanol and stored in a desiccator over CaCl<sub>2</sub>. Crystals suitable for X-ray crystallography were grown by liquid-liquid diffusion [23,24] using water as solvent and ethanol as precipitant. Crystal analysis: Na<sub>4</sub>[Co<sub>2</sub>(*p*-PhDTA)<sub>2</sub>] · 8H<sub>2</sub>O (pinkish violet) Found: C, 32.5; H, 3.4; N, 5.2; Co, 10.8. Calc.

Table 3. Formation constants ( $\log \beta_{pqr}$ ) for *p*-PhDTA acid with Ni<sup>II</sup>, Co<sup>II</sup>, Zn<sup>II</sup> and Cd<sup>II</sup> (25°C;  $I = 0.1 \text{ mol dm}^{-3}$ , ligand H<sub>4</sub>L)

<i>pqr</i>	Species	Ni <sup>IIa</sup>	Co <sup>IIb</sup>	Zn <sup>IIc</sup>	Cd <sup>II d</sup>
211	[H <sub>2</sub> ML]	13.72 ± 0.05	13.30 ± 0.08	13.85 ± 0.09	13.19 ± 0.22
111	[HML] <sup>-</sup>	10.87 ± 0.03	Max. 9.29	Max. 9.33	9.24 ± 0.10
011	[ML] <sup>2-</sup>	Max. 5.75	Max. 5.66	Max. 5.31	3.98 ± 0.20
222	[H <sub>2</sub> M <sub>2</sub> L <sub>2</sub> ] <sup>2-</sup>	—	Max. 22.99	Max. 23.83	Max. 22.01
122	[HM <sub>2</sub> L <sub>2</sub> ] <sup>3-</sup>	20.11 ± 0.17	19.58 ± 0.22	19.84 ± 0.23	Max. 17.17
022	[M <sub>2</sub> L <sub>2</sub> ] <sup>4-</sup>	Max. 15.64	15.72 ± 0.19	Max. 15.46	Max. 11.86
133	[HM <sub>3</sub> L <sub>3</sub> ] <sup>5-</sup>	—	—	Max. 29.73	—
033	[M <sub>3</sub> L <sub>3</sub> ] <sup>6-</sup>	—	26.09 ± 0.07	Max. 25.77	Max. 20.03
044	[M <sub>4</sub> L <sub>4</sub> ] <sup>8-</sup>	—	—	—	—
055	[M <sub>5</sub> L <sub>5</sub> ] <sup>10-</sup>	44.64 ± 0.15	—	—	—
066	[M <sub>6</sub> L <sub>6</sub> ] <sup>12-</sup>	Max. 54.03	Max. 54.68	—	—
021	[M <sub>2</sub> L]	9.35 ± 0.25	Max. 9.06	Max. 9.14	Max. 7.38
032	[M <sub>3</sub> L] <sup>2-</sup>	—	Max. 18.83	—	—
043	[M <sub>4</sub> L] <sup>4-</sup>	29.30 ± 0.12	Max. 28.99	—	—
412	[H <sub>4</sub> ML <sub>2</sub> ] <sup>2-</sup>	—	Max. 26.27	27.22 ± 0.24	—
312	[H <sub>3</sub> ML <sub>2</sub> ] <sup>3-</sup>	23.86 ± 0.16	23.78 ± 0.10	24.02 ± 0.09	23.14 ± 0.23
212	[H <sub>2</sub> ML <sub>2</sub> ] <sup>4-</sup>	20.85 ± 0.03	20.66 ± 0.04	20.74 ± 0.06	Max. 18.88
112	[HML <sub>2</sub> ] <sup>5-</sup>	15.98 ± 0.06	16.31 ± 0.07	Max. 16.30	13.99 ± 0.19
012	[ML <sub>2</sub> ] <sup>6-</sup>	10.59 ± 0.03	10.97 ± 0.07	—	8.56 ± 0.15
123	[HM <sub>2</sub> L <sub>3</sub> ] <sup>7-</sup>	Max. 25.40	—	—	—
134	[HM <sub>3</sub> L <sub>4</sub> ] <sup>9-</sup>	Max. 35.34	Max. 35.78	—	—

Polymerization equilibria,  $\log K$  values ( $I = 0.1 \text{ mol dm}^{-3}$ )

Equilibria	Cu <sup>II</sup>	Ni <sup>II</sup>	Co <sup>II</sup>	Zn <sup>II</sup>	Cd <sup>II</sup>
(9) 2[MHL] <sup>-</sup> ⇌ [H <sub>2</sub> M <sub>2</sub> L <sub>2</sub> ] <sup>2-</sup>	1.71	—	4.41	5.17	3.53
(10) 2[ML] <sup>2-</sup> ⇌ [M <sub>2</sub> L <sub>2</sub> ] <sup>4-</sup>	3.80	4.14	4.40	4.84	3.90
(11) 3[ML] <sup>2-</sup> ⇌ [M <sub>3</sub> L <sub>3</sub> ] <sup>6-</sup>	8.02	—	9.11	9.84	8.09
(12) 5[ML] <sup>2-</sup> ⇌ [M <sub>5</sub> L <sub>5</sub> ] <sup>10-</sup>	15.82	15.89	—	—	—
(13) 2[M <sub>3</sub> L <sub>3</sub> ] <sup>6-</sup> ⇌ [M <sub>6</sub> L <sub>6</sub> ] <sup>12-</sup>	2.90	—	2.50	—	—

<sup>a</sup> 14 titrations (ratio 1 : 1,  $C_M = 1, 2, 4, 6, 10, 15, 20, 30$  and  $50 \times 10^{-3} \text{ mol dm}^{-3}$ ; L : M, 1 : 3,  $C_M = 3$  and  $4.5 \times 10^{-3} \text{ mol dm}^{-3}$ ; L : M, 3 : 1,  $C_M = 1, 1.5$  and  $2 \times 10^{-3} \text{ mol dm}^{-3}$ ); 384 points;  $[\sigma(Z)] = 0.039$ ;  $-\log[H^+]$  range 2.70–6.15.

<sup>b</sup> 16 titrations (ratio 1 : 1,  $C_M = 0.3, 0.5, 0.7, 1, 4, 6, 10, 15, 20$  and  $30 \times 10^{-3} \text{ mol dm}^{-3}$ ; L : M, 1 : 3,  $C_M = 3, 4.6$  and  $6 \times 10^{-3} \text{ mol dm}^{-3}$ ; L : M, 3 : 1,  $C_M = 1, 1.6$  and  $2 \times 10^{-3} \text{ mol dm}^{-3}$ ); 534 points;  $\sigma(Z) = 0.050$ ;  $-\log[H^+]$  range 2.71–5.86.

<sup>c</sup> Five titrations (ratio 1 : 1,  $C_M = 0.4, 0.5$  and  $0.8 \times 10^{-3} \text{ mol dm}^{-3}$ ; L : M, 3 : 1,  $C_M = 0.5$  and  $0.8 \text{ mol dm}^{-3}$ ); 103 points;  $\sigma(Z) = 0.033$ ;  $-\log[H^+]$  range 2.87–4.05.

<sup>d</sup> Four titrations (ratio 1 : 1,  $C_M = 0.4, 0.5, 0.8$  and  $1.0 \times 10^{-3} \text{ mol dm}^{-3}$ ); 81 points;  $\sigma(Z) = 0.025$ ;  $-\log[H^+]$  range 3.21–5.84.

for C<sub>28</sub>H<sub>40</sub>N<sub>4</sub>O<sub>24</sub>Co<sub>2</sub>Na<sub>4</sub>: C, 32.8; H, 3.9; N, 5.5; Co, 11.5%. Elemental analyses were performed on a Carlo Erba 1106 automatic analyser. Cobalt was determined by atomic absorption.

#### X-ray structure determination

Many of the details of the structure analysis are listed in Table 4. X-ray diffraction measurements were made using a Nonius CAD-4 diffractometer. Cell dimensions were determined from 25 centred reflections ( $9 < \theta < 19^\circ$ ). The structure was solved by Patterson synthesis, using the SHELXS-86 computer

program [25] and refinement by full-matrix least-squares method, using the SHELXL-93 computer program [26]. Refinement was made on  $F^2$  for all reflections except for zero with very negative  $F^2$  or flagged by the user for potential systematic errors. Weighted  $R$ -factors,  $wR$ , and all goodnesses of fit  $S$  values are based on  $F^2$ , conventional  $R$ -factors  $R$  are based on  $F$ , with  $F$  set to zero for negative  $F^2$ . The observed criterion of  $F^2 > 2\sigma(F^2)$  is used only for calculating the  $R$  factor observed, etc. and is not relevant to the choice of reflections for refinement. Reflections were weighted according to the formula  $w = 1/[\sigma^2(F_o^2) + 250 + (0.0976P)^2]$ , where  $P = (F_o^2 + 2F_c^2)/3$ . The position of the hydrogen atoms was computed and refined with an overall isotropic temperature factor.

Table 4. Crystal data and structure refinement for  $\text{Na}_4[\text{Co}_2(\text{p-PhDTA})_2] \cdot 8\text{H}_2\text{O}$ 

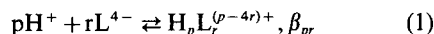
Empirical formula	$\text{C}_{28}\text{H}_{40}\text{Co}_2\text{N}_4\text{Na}_4\text{O}_{24}$
Formula weight	1026.46
Temperature (K)	293(2)
Radiation	Mo- $K_\alpha$ (0.71069 Å)
Crystal system	Orthorhombic
Space group	$Pcab$
$a$ (Å)	22.127(6)
$b$ (Å)	22.119(6)
$c$ (Å)	15.895(4)
$\alpha = \beta = \gamma$ (°)	90(—)
Volume (Å <sup>3</sup> )	7779(4)
$Z$	8
$D_0$ (g cm <sup>-3</sup> )	1.753
Absorption coefficient (mm <sup>-1</sup> )	0.998
$F(000)$	4208
Crystal size (mm)	0.80 × 0.40 × 0.20
$\theta$ range (°)	1.83 to 24.98
Index ranges	$0 \leq h \leq 26, 0 \leq k \leq 26, 0 \leq l \leq 18$
Reflections collected	6833
Independent reflections	6833 ( $R_{\text{int}} = 0.0000$ )
Refinement method	Full-matrix least-squares on $F^2$
Data/restraints/parameters	6833/406/560
Goodness-of-fit on $F^2$	0.811
Final $R$ indices [ $I > 2\sigma(I)$ ]	$R_1 = 0.0481, wR_2 = 0.1295$
$R$ indices (all data)	$R_1 = 0.1425, wR_2 = 0.1523$
Largest difference peak and hole (e Å <sup>-3</sup> )	0.590 and -0.618

Atomic scattering factors and anomalous-dispersion corrections for all atoms were taken from International Tables for Crystallography [27].

## RESULTS AND DISCUSSION

### Ionization constants of the acid

From the values obtained for the constants  $\beta_{pr}$  corresponding to the equilibrium (1) (ligand  $\text{H}_4\text{L}$ ):



the ionization constants of the acid,  $K_i$ , given in Table 1, for both 0.5 and 0.1 mol dm<sup>-3</sup> in KCl ionic media, could readily be determined. The values of  $\text{p}K_i$  obtained from the monosodium salt of *p*-PhDTA acid ( $\text{NaH}_3\text{L}$ ) are more accurate than those obtained from *p*-PhDTA acid [6] since the salt is more easily obtained with a greater degree of purity. For comparison purposes, values for 2,5-TDTA acid [28] are also included.

The values of  $\text{p}K_0$ ,  $\text{p}K_1$  and  $\text{p}K_2$  correspond to protons situated fundamentally over carboxylic groups, whereas the values of  $\text{p}K_3$  and  $\text{p}K_4$  correspond to fundamentally betainic protons [21,22]. The order of basicity for the species  $\text{HL}^{3-}$ , 2,5-TDTA > *p*-PhDTA is explained by the inductive electron-donor nature of the radical  $\text{CH}_3$ . The species distribution diagram as

a function of  $\text{pH}$  ( $= -\log [\text{H}^+]$ ) is presented in Fig. 1. The diprotonated  $\text{H}_2\text{L}^{2-}$  species, with the betainic protons [21,22], has the largest field of existence and is the most important at  $\text{pH}$  3.0–4.8.

### Formation constants of the complexes formed

The analysis of the experimental data by means of NERNST/LETA [15] allowed the calculation of  $\beta_{pr}$

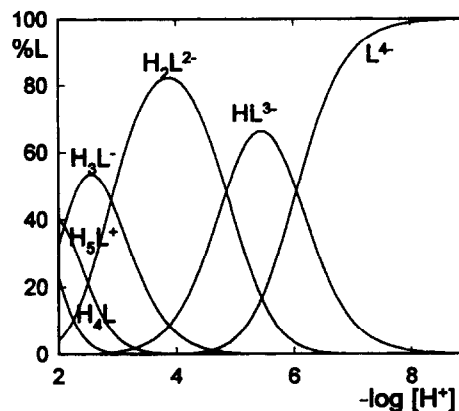
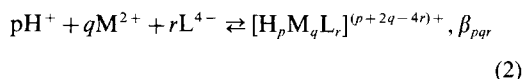


Fig. 1. Species distribution diagram as a function of  $-\log[\text{H}^+]$  for the *p*-PhDTA acid. Calculated from the values of  $\beta_{pr}$  given in Table 1 ( $I = 0.1$  M in KCl).

formation constants for the complex species formed, defined by means of the equilibrium (2):



which are given in Table 2 for  $\text{Cu}^{\text{II}}$  and Table 3 for  $\text{Ni}^{\text{II}}$ ,  $\text{Co}^{\text{II}}$ ,  $\text{Zn}^{\text{II}}$  and  $\text{Cd}^{\text{II}}$ .

(a) *Analysis of the Z(pH) curves: identification of the polymer complex species.* In accord with the reaction scheme (2), the function Z is defined as the mean number of  $\text{H}^+$  ions bound by a/the central metal ion, according to expression (3):

$$Z = \frac{C_{\text{H}} - [\text{H}^+]}{C_{\text{M}}} = \frac{\sum p \cdot \text{H}_p\text{M}_q\text{L}_r + \sum i \cdot \text{H}_i\text{L}}{C_{\text{M}}} \quad (3)$$

where  $C_{\text{H}}$  and  $C_{\text{M}}$  represent the total concentrations of  $\text{H}^+$  and metal.

Taking as an example the experimental Z(pH) data for the  $\text{Co}^{\text{II}}-p\text{-PhDTA}$  system in the ratio 1:1, at  $C_{\text{M}} = 0.5, 1, 4, 10$  and 20 mM (Fig. 2). It is observed that as the concentration of metal increases, the curves are shifted to the left, implying an increase in the concentration of  $\text{H}^+$  and of Z. It is well known that in the hydrolysis of cations [29] and in the polymerization of anions (two-component systems), the Z(pH) curves for different total concentrations of metal will only coincide if mono- or homonuclear complexes are formed; in the case of homonuclear complexes, the curves will be independent of the total concentration of metal only when the concentration of free metallic ion is negligible in comparison with that of the complexes formed. However, in the case of the formation of polynuclear complexes, when the concentration of metal and Z increase, the pH decreases [29], as observed in the shift of the Z(pH) curves with the total concentration of metal. This issue has been discussed in depth by Sillén [30] and co-

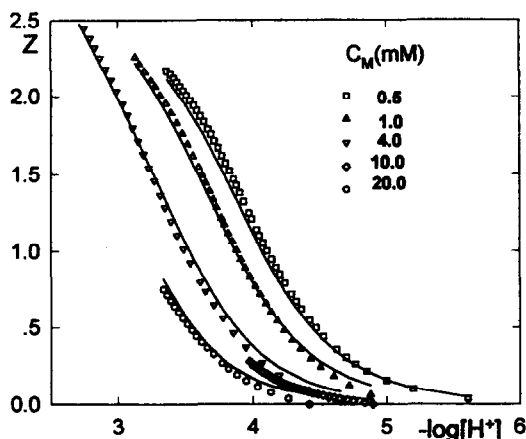


Fig. 2. Z(-log[H<sup>+</sup>]) curves for the  $\text{Co}^{\text{II}}-p\text{-PhDTA}$  system ( $I = 0.1$  M in KCl). Ligand:metal ratio 1:1;  $C_{\text{M}} = 0.5, 1, 4, 10$  and 20 mM. Full curves calculated from the values of  $\beta_{pr}$  (Table 1) and  $\beta_{pqr}$  (Table 3).

workers [31], and is currently included in the teaching program of Advanced Courses in Equilibria in Solution [32,33].

For the case of a three-component system we have attempted to simulate a similar situation. Firstly, let us imagine a mononuclear system formed by the complexes ML, HML and  $\text{H}_2\text{ML}$ . If the complexes are very stable the Z(pH) curves, ligand:metal ratio = 1:1, coincide for any concentration of metal, Fig. S1a, because in equation (3) the term  $\sum i\text{H}_i\text{L}$  is practically negligible. However, the weaker the complexes, the more significant the term  $\sum i\text{H}_i\text{L}$ , such that for weak complexes the curves do not coincide, Fig. S1b, shifting further to the left, the greater the concentration of metal. In other words, the fact that the Z(pH) curves do not coincide, does not always imply the formation of polynuclear complexes in three-component systems. However, it can be observed that Fig. S1b is very different from Fig. 2. In order to verify if this different is due to the formation of polynuclear species, by means of the program NERNST/LETA [15], we carried out the following simulations:

(1) If in addition to the formation of the very stable monomers ML, HML and  $\text{H}_2\text{ML}$ , very stable dimers,  $\text{M}_2\text{L}_2$ ,  $\text{HM}_2\text{L}_2$  and  $\text{H}_2\text{M}_2\text{L}_2$ , are formed, the Z(pH) curves will no longer coincide as the concentration of metal increases, when the dimerization equilibrium  $2\text{H}_i\text{ML} \rightleftharpoons \text{H}_{2i}\text{M}_2\text{L}_2$  shifts towards the right, because in that case the acidity corresponding to the term  $\sum p \cdot \text{H}_p\text{M}_q\text{L}_r$  increases [eq. (3)] the pH decreases and Z increases, that is, the curves shift to the left, Fig. S1c. This situation is valid for any process of polymerization  $n\text{H}_i\text{ML} \rightleftharpoons \text{H}_n\text{M}_n\text{L}_n$  shifted towards the right. It should be noted that the non-protonated complexes  $\text{M}_n\text{L}_n$  predominate when  $Z = 0$  and that Z increases as the pH diminishes, as a consequence of the acidification reactions  $\text{M}_n\text{L}_n + i\text{H} \rightleftharpoons \text{H}_i(\text{ML})_n$  (Figs S1c, S1d and 2).

(2) If the polymer complexes are weaker, but the polymerization reaction  $n\text{H}_i\text{ML} \rightleftharpoons \text{H}_n\text{M}_n\text{L}_n$  is shifted to the right, the displacement of the curves towards the left, as the concentration of metal increases, is similar and this shift is greater the larger the stability constants of the polymer species. Figure S1d shows that with monomers, dimers, trimers, pentamers and hexamers having formation constant values close to the final calculated values (Table 3), a family of curves of Z(pH) is obtained that resembles those of Fig. 2, confirming the formation of the polymer species, although the complexes with excess of ligand and excess of metal have not been taken into account in the simulation. Indeed, the analysis of the experimental data by means of the LETAGROP program indicates that the best fit of the experimental data (Figs 2-4) is obtained by supposing the formation of the set of complex species given in Tables 2 and 3. The full curves in Fig. 2 show the position of the best fit for  $\text{Co}^{\text{II}}$ . In order to achieve this fit the following procedure was followed: the curves in the ratio 1:1 were first analysed, followed by the analysis of the

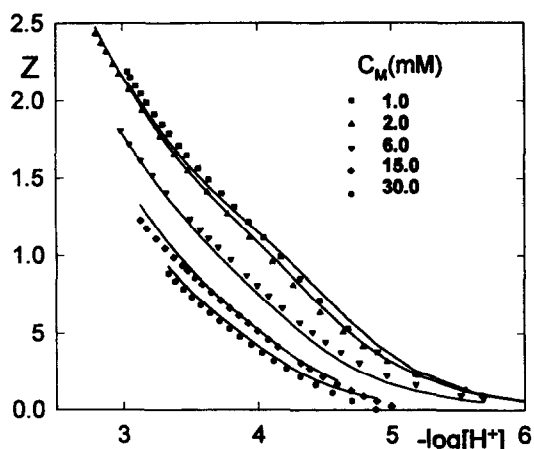


Fig. 3.  $Z(-\log[H^+])$  curves for the  $\text{Ni}^{\text{II}}$ -*p*-PhDTA system ( $I = 0.1 \text{ M}$  in KCl). Ligand:metal ratio 1:1;  $C_M = 1, 2, 6, 15$  and  $30 \text{ mM}$ . Full curves calculated from the values of  $\beta_{pr}$  (Table 1) and  $\beta_{par}$  (Table 3).

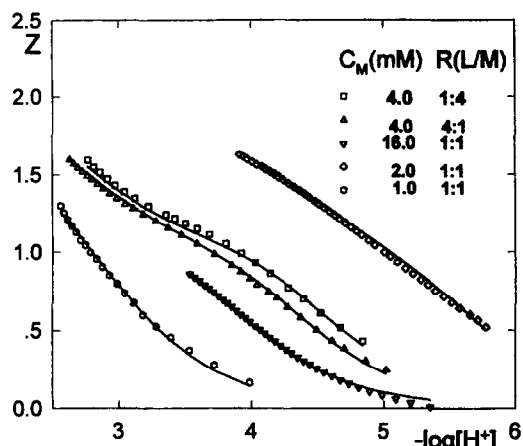


Fig. 4.  $Z(-\log[H^+])$  curves for the  $\text{Cu}^{\text{II}}$ -*p*-PhDTA system ( $I = 0.5 \text{ M}$  in KCl). Ligand:metal ratio 1:1 ( $C_M = 1, 2$  and  $16 \text{ mM}$ ); 4:1 ( $C_M = 4 \text{ mM}$ ); 1:4 ( $C_M = 4 \text{ mM}$ ). Full curves calculated from the values of  $\beta_{pr}$  (Table 1) and  $\beta_{par}$  (Table 2).

curves with excess of ligand and with excess of metal, respectively. Finally, all the data were treated simultaneously. A behaviour similar to that of the system  $\text{Co}^{\text{II}}$ -*p*-PhDTA was presented by the systems  $\text{Ni}^{\text{II}}$ -*p*-PhDTA (Fig. 3) and  $\text{Cu}^{\text{II}}$ -*p*-PhDTA (Fig. S2). The results obtained are also given in Table 2 for  $\text{Cu}^{\text{II}}$  and Table 3 for  $\text{Ni}^{\text{II}}$ . In Fig. 4 the data of the system  $\text{Cu}^{\text{II}}$ -*p*-PhDTA in KCl  $0.5 \text{ mol dm}^{-3}$ , are plotted both in the ligand:metal ratio 1:1 and with excess of ligand 4:1 and excess of metal 1:4. In Table 2 it is observed that the values of the formation constants at both  $I = 0.1$  and  $0.5 \text{ mol dm}^{-3}$  are practically the same. A good agreement is also observed between the model calculated with the values of the formation constants (Table 2) and the experimental data (Figs S2 and 4, respectively). Satisfactory fits are also obtained for the systems  $\text{Zn}^{\text{II}}$ -*p*-PhDTA (Fig. S5) and  $\text{Cd}^{\text{II}}$ -*p*-PhDTA (Fig. S6). In the LETAGROP program [16], when the error of the formation constant is  $< 20\%$ ,

the constant  $\beta_{par}$  is expressed in the form:

$$\log \beta_{par} \pm 3\sigma (\log \beta_{par}) \text{ (constant well defined)}$$

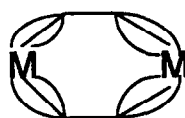
whereas when the complex species is present in small amounts and the error is  $> 20\%$ , the constant is expressed in the form:

$\log \beta_{par}$  ( $<$  maximum value) (constant not well defined). (Tables 2 and 3).

In Table 3 for the cations studied, the constants corresponding to the polymerization equilibria are also summarized. The polymer complex species have been identified for the first time in aqueous solution using emf methods. For the monomer complexes  $\text{MH}_2\text{L}$  and  $\text{MHL}^-$  the values found for  $\log K$  are in good agreement with those previously found in the same ionic medium and temperature [4,5], but  $\log K$  for the complexes  $\text{ML}^{2-}$  is more affected by the presence of polymer species.

(b) *Species distribution diagrams as a function of  $-\log [H^+]$ .* The species distribution diagrams for each cation are calculated to take into account the values of  $\beta_{pr}$  of the ligand (Table 1) and the values of  $\beta_{par}$  of the complexes (Tables 2 and 3).

In the ratio  $R : 1 : 1$  the diagrams (Fig. 5 for  $\text{Cu}^{\text{II}}$ , Fig. 7(a) and S3b for  $\text{Ni}^{\text{II}}$ , Fig. 8(b) and S4a for  $\text{Co}^{\text{II}}$ , Fig. S5 for  $\text{Zn}^{\text{II}}$  and Fig. S6 for  $\text{Cd}^{\text{II}}$ ) indicate that at  $\text{pH} > 5$  the trimer complex  $[\text{M}_3\text{L}_3]^{6-}$  is the more important polymer complex for  $\text{Cu}^{\text{II}}$ ,  $\text{Co}^{\text{II}}$ ,  $\text{Zn}^{\text{II}}$  and  $\text{Cd}^{\text{II}}$ , whereas for  $\text{Ni}^{\text{II}}$  it is the pentamer complex  $[\text{M}_5\text{L}_5]^{10-}$ , which is also important for  $\text{Cu}^{\text{II}}$ . The hexamer complex  $[\text{M}_6\text{L}_6]^{12-}$  is not well defined for  $\text{Cu}^{\text{II}}$ ,  $\text{Ni}^{\text{II}}$  and  $\text{Co}^{\text{II}}$  (Tables 2 and 3), but the diagrams show that the percentage is increased with the concentration as expected. In general at  $\text{pH} < 5$ , the protonated complexes are more important than the non-protonated complexes [see  $Z(\text{pH})$  curves, Figs 2–4, Tables 2–3 and diagrams, Figures 5–8 and S3–S6]. The dimer non-protonated which is better defined (Tables 2 and 3) is  $[\text{Co}_2\text{L}_2]^{4-}$ . Precisely, although Figs 8 and S4 shows that at  $\text{pH} > 5$  the trimer  $[\text{Co}_3\text{L}_3]^{6-}$  is present in greater percentage than the dimer  $[\text{Co}_2\text{L}_2]^{4-}$ , from a concentrated aqueous solution at ligand:metal ratio 2:3 at  $\text{pH} 5$  (see the Experimental, preparation of the dimer complex) we obtained suitable crystals for X-ray crystallography of the dimer complex  $[\text{Co}_2\text{L}_2]^{4-}$  (Fig. 9) and not of the trimer complex  $[\text{Co}_3\text{L}_3]^{6-}$ , probably due to solubility effects. Since the dimer  $[\text{Co}_2\text{L}_2]^{4-}$  has a closed structure (Fig. 9) with both  $\text{Co}^{\text{II}}$  atoms bonded to two iminodiacetate groups, we believe that the trimer complex will also have a cyclical closed structure in order to saturate each  $\text{Co}^{\text{II}}$  atom with two iminodiacetate groups (ligand:metal ratio 1:1):



dimer complex



trimer complex  
non protonated polymer complexes (ratio 1:1)

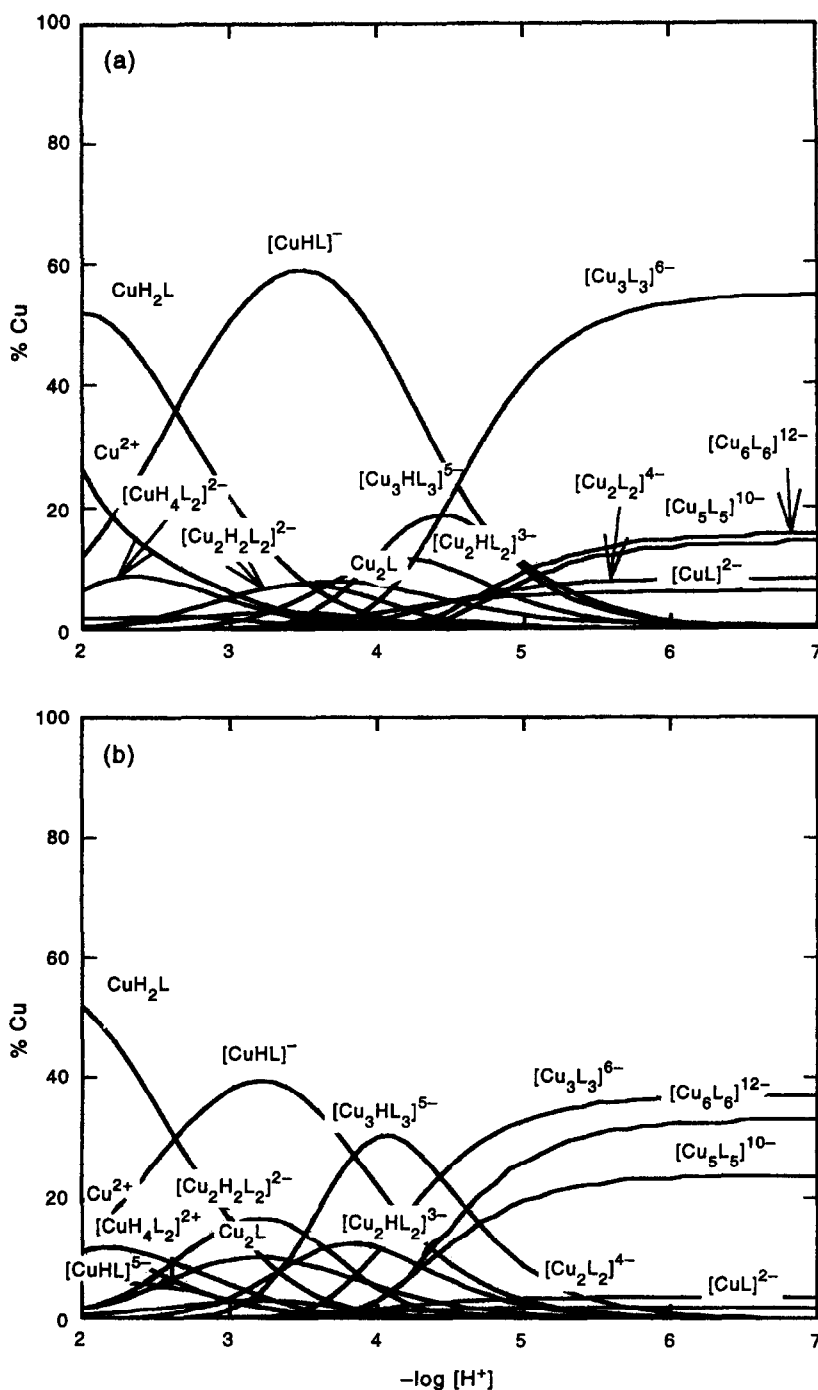


Fig. 5. Species distribution diagram as a function of  $-\log[H^+]$  for the  $\text{Cu}^{\text{II}}$ -*p*-PhDTA system ( $I = 0.5 \text{ mM}$  in KCl). Ligand: metal ratio 1 : 1: (a)  $C_M = 2 \text{ mM}$ ; (b)  $C_M = 10 \text{ mM}$ .

The pentamer and hexamer complexes also possibly have the cyclic closed structure.

Up to the present time we have not obtained suitable crystals for X-ray crystallography of the trimer, pentamer and hexamer complexes of  $\text{Cu}^{\text{II}}$ ,  $\text{Ni}^{\text{II}}$  and  $\text{Co}^{\text{II}}$ . The complexes of  $\text{Zn}^{\text{II}}$  and  $\text{Cd}^{\text{II}}$  precipitate at  $C_M > 1 \times 10^{-3} \text{ mol dm}^{-3}$ . However, at  $C_M = 1 \times 10^{-3} \text{ mol dm}^{-3}$  (ratio 1 : 1) a small proportion of dimer complexes is found and the trimer complexes are

important specially for  $\text{Zn}^{\text{II}}$  (Table 3, Figs S5 and S6). The dimer  $[\text{HZn}_2\text{L}_2]^{3-}$  is well defined (Table 3). The values of  $\log K$  for the polymerization equilibria (9)–(13) (Table 3) indicate that the equilibria are displaced to the right and the percentage of the polymer species is increased with the concentration (Figs 5, 7, 8, S3 and S4).

The complex with excess of metal  $\text{M}_2\text{L}$  is well defined for  $\text{Cu}^{\text{II}}$  [Table 2, Fig. 6(a)]. The crystal struc-



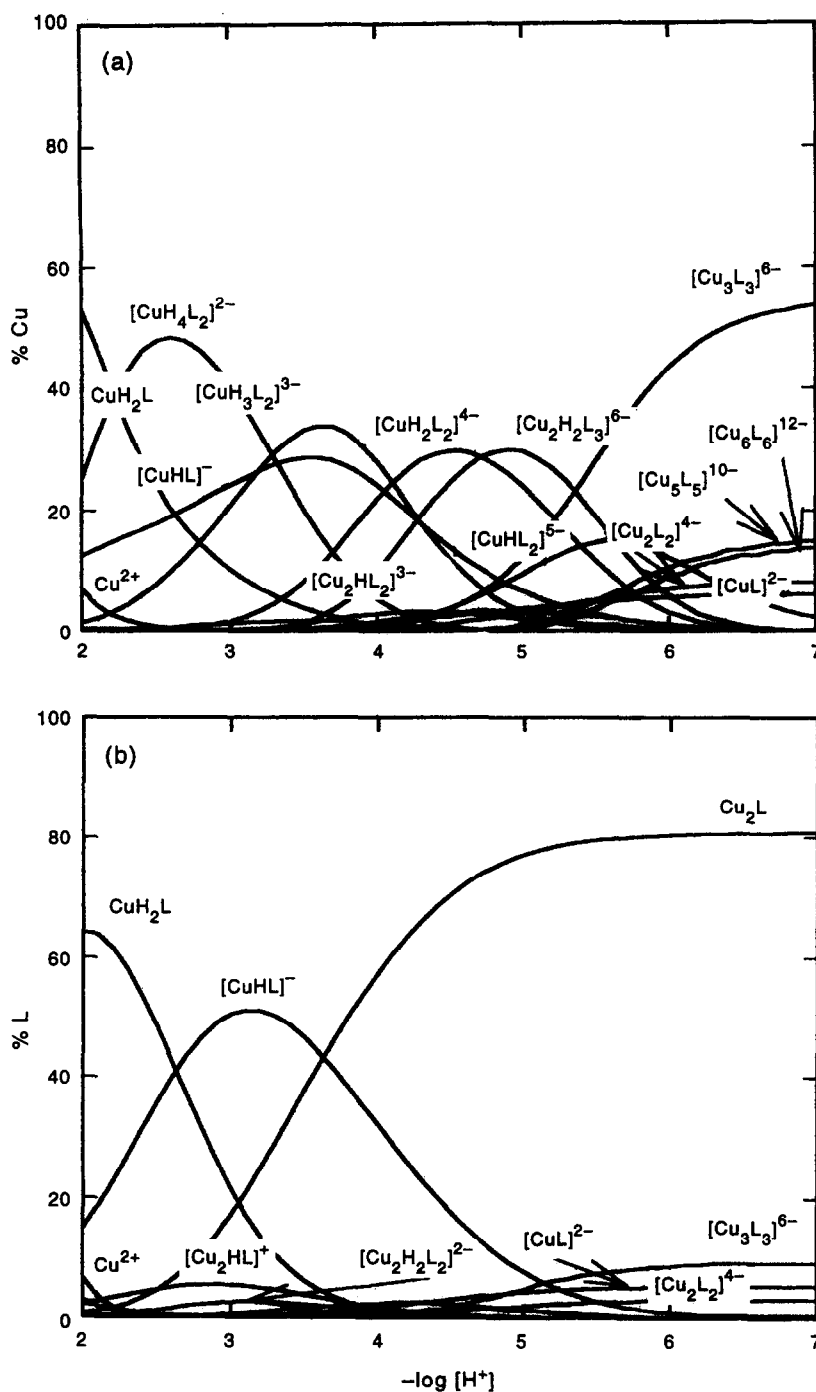


Fig. 6. Species distribution diagram as a function of  $-\log[H^+]$  for the  $\text{Cu}^{\text{II}}$ -*p*-PhDTA system at  $C_M = 2 \text{ mM}$  ( $I = 0.5 \text{ M}$  in KCl). Ligand: metal ratio: (a) 2:1, %Cu; (b) 1:2, %L.

ture of the complex  $\text{Cu}_2(\textit{p}\text{-PhDTA})$  has been determined previously [2]. However, for  $\text{Ni}^{\text{II}}$  and  $\text{Co}^{\text{II}}$  the diagrams [Fig. 7(b) for  $\text{Ni}^{\text{II}}$  and Fig. S4b for  $\text{Co}^{\text{II}}$ ] indicate that the polymer complex  $[\text{M}_4\text{L}_3]^{4-}$  is more important than the bimetallic complex  $\text{M}_2\text{L}$ . For  $\text{Ni}^{\text{II}}$ , the complexes  $[\text{Ni}_4\text{L}_3]^{4-}$  and  $\text{Ni}_2\text{L}$  are well defined (Table 3).

The complexes with excess ligand, ratio 2:1, are in

general well defined for all cations, but  $[\text{CuL}_2]^{6-}$  [Table 2, Fig. 6(a)] are not present. However,  $[\text{CoL}_2]^{6-}$  and  $[\text{NiL}_2]^{6-}$  are very important at  $\text{pH} > 5$  [Table 3, Figs 8(a) and S3a, respectively]. In these complexes, the metal is bonded to two iminodiacetate groups from different ligands. Other polymer complexes with excess of ligand are not well defined at the concentrations and ligand: metal ratios studied.

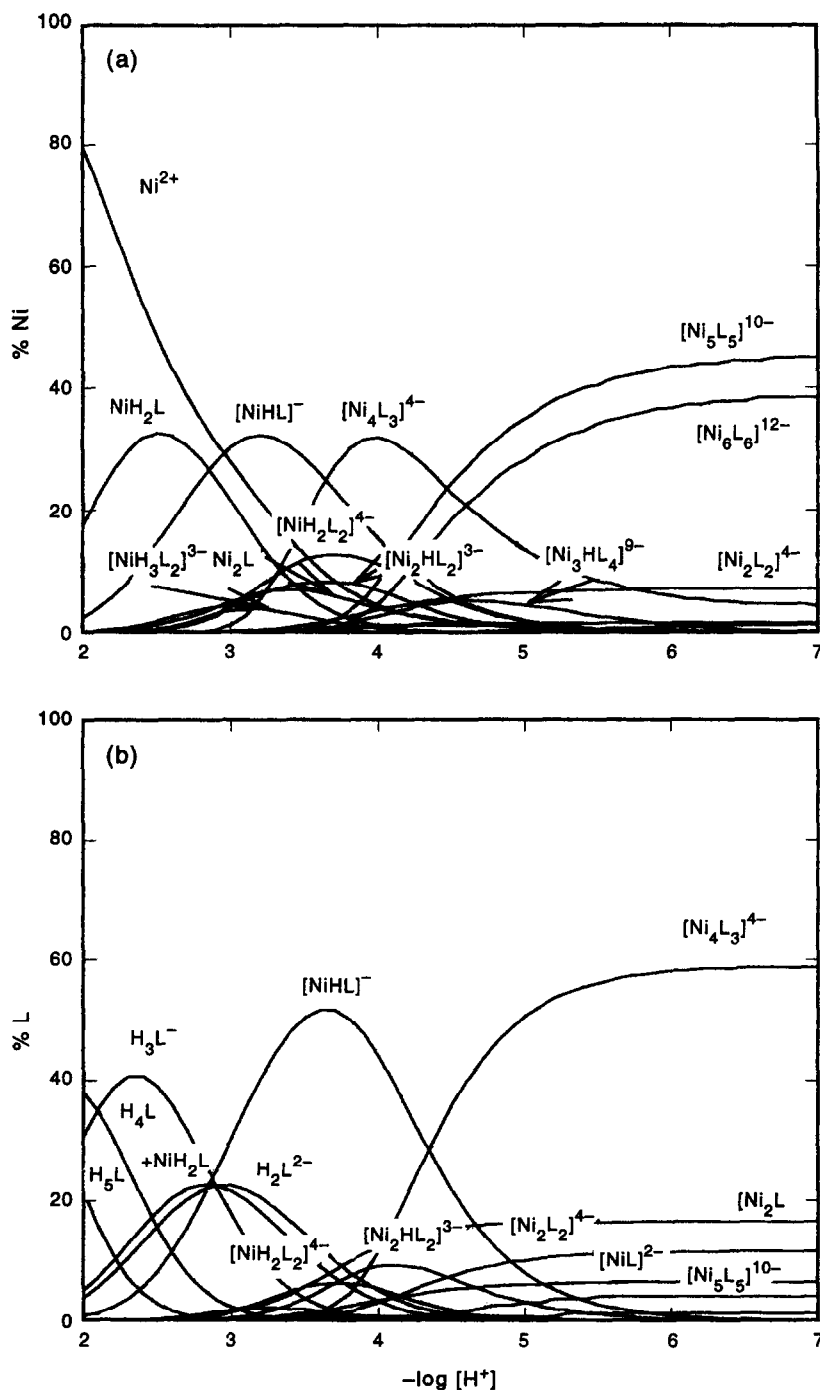


Fig. 7. Species distribution diagram as a function of  $-\log[H^+]$  for the  $Ni^{II}$ -*p*-PhDTA system ( $I = 0.1$  M in KCl): (a) ligand : metal ratio 1 : 1,  $C_M = 10$  mM, %Ni; (b) ligand : metal ratio 1 : 2,  $C_M = 2$  mM, %L.

In Tables 2 and 3 we can see that the Irving and Williams order of complexation  $Co^{II} < Ni^{II} < Cu^{II} > Zn^{II}$  is fulfilled by all complexes. The Irving-Williams order is related to the ligand-field stabilization energies. As in the dimer complex  $[Co_2(p\text{-PhDTA})_2]^{4-}$  (Fig. 9), in the polymer complexes (Scheme) each metal is bonded to two iminodiacetate groups with hexa-coordination approximately

octahedra. In the monomer complexes and in complexes with excess metal, the metal is only coordinated to one iminodiacetic group to complete the coordination with molecules of solvent in monomers and also with oxygen atoms of other carboxylate groups complexed in complexes with excess of metal, as in the complex [2]  $[Cu_2(p\text{-PhDTA})(H_2O)_4] \cdot 2H_2O$ .

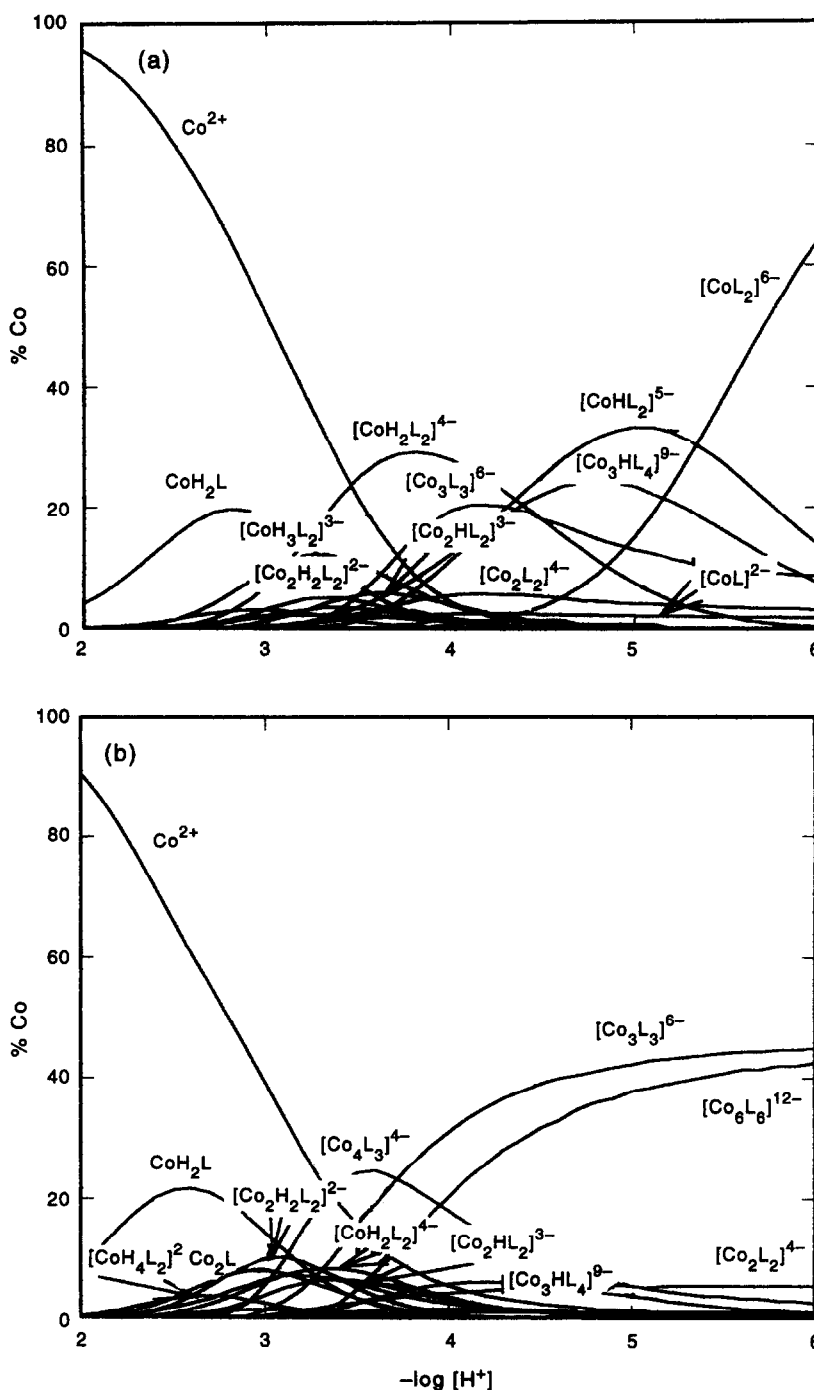


Fig. 8. Species distribution diagram as a function of  $-\log [H^+]$  for the  $Co^{II}$ -*p*-PhDTA system ( $I = 0.1$  M in KCl): (a) ligand : metal ratio 2 : 1,  $C_M = 2$  mM, %Co; (b) ligand : metal ratio 1 : 1,  $C_M = 10$  mM, %Co.

*Description of the complex  $Na_4[Co_2(p\text{-PhDTA})_2] \cdot 8H_2O$*

The selected bond distance and angles are given in Table 5. Additional structural information is given as supplementary material.

An ORTEP drawing [35] of the complex with the

atomic numbering scheme employed for all non hydrogen atoms is shown in Fig. 9.

Crystals of this compound consist of sodium coordinated cations (Fig. 10), binuclear cobalt anions (Fig. 9) and four non-coordinated water molecules of crystallization.

For *m*-PhDTA acid [9], the dimeric anion  $[Co_2(m$

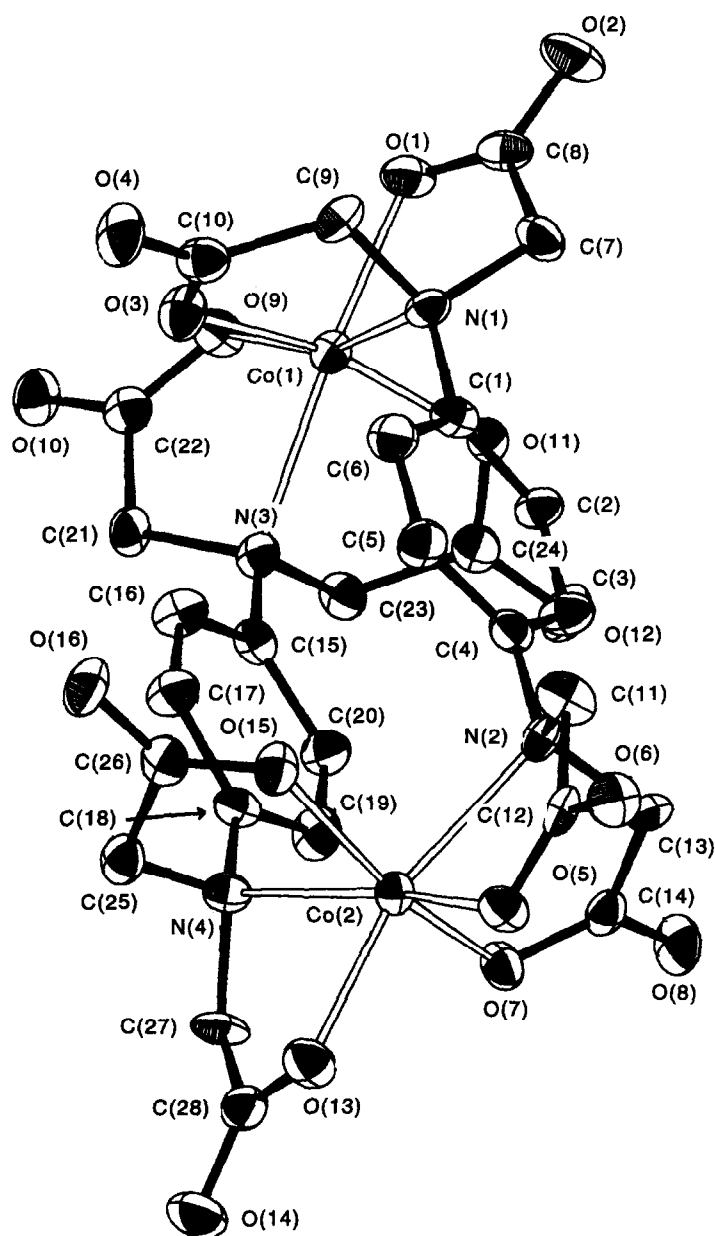


Fig. 9. ORTEP view of the anionic complex  $[\text{Co}_2(p\text{-PhDTA})_2]^{4-}$  (50% probability ellipsoids; H atoms excluded).

$\text{PhDTA}]_2^{4-}$  is centrosymmetric  $C_i$ , with each metal atom surrounded by four carboxylic oxygens and two amine nitrogens from two iminodiacetate groups of different *m*-PhDTA ligands, in a distorted octahedron. The structure of the dimeric anion  $[\text{Co}_2(p\text{-PhDTA})_2]^{4-}$  is similar, but the symmetry  $C_i$  is lost (Fig. 9), probably due to the *para* position of the nitrogen atoms. In the *m*-PhDTA complex, the benzenic rings are parallel (distance 3.59 Å), while in the *p*-PhDTA complex (Fig. 9) a light deviation is present [ $3.0(2)^\circ$ ] with a distance between 3.61 and 3.74 Å [for C(16) and C(18), respectively].

The cobalt atoms have a distorted octahedral structure with the two nitrogen atoms occupying relative

*cis* positions (see Table 5). The N—Co—N angles have a high value [118.6(2) and 117.4(2) $^\circ$ , respectively], Table 5, very near to the value for the  $[\text{Co}_2(m\text{-PhDTA})]^{4-}$  complex [9] [116.3(1) $^\circ$ ], but higher than those reported for analogous complexes containing *ortho*-substituted EDTA-like ligands, i.e. 84.3(1) $^\circ$  for  $[\text{Co}(\text{EDTA})]^{2-}$  [36], 79.96(7) $^\circ$  for  $[\text{Co}(o\text{-PhDTA})]^{2-}$  (*o*-PhDTA = *ortho*-phenylenediamine-*N,N,N',N'*-tetraacetic acid) [36] and 79.1(1) $^\circ$  for  $[\text{Co}(4\text{-Cl-}o\text{-PhDTA})]^{2-}$  (4-Cl-*o*-PhDTA = 4-chloro-1,2-phenylenediamine-*N,N,N',N'*-tetraacetic acid) [37]. This circumstance is probably due to the stronger geometric constraints existing in the latter complexes that force both nitrogens to be coordinated to the

Table 5. Selected bond distances (Å) and angles (°) for Na<sub>4</sub>[Co<sub>2</sub>(*p*-PhDTA)<sub>2</sub>]·8H<sub>2</sub>O with estimated standard deviations (e.s.d.s) in parentheses

<b>(a) Coordination sphere of cobalt</b>			
Co(1)—O(11)	2.026(4)	Co(1)—O(3)	2.030(4)
Co(1)—O(1)	2.053(4)	Co(1)—O(9)	2.064(4)
Co(1)—N(1)	2.291(4)	Co(1)—N(3)	2.308(4)
Co(2)—N(4)	2.297(4)	Co(2)—O(13)	2.054(4)
Co(2)—O(15)	2.033(4)	Co(2)—O(7)	2.025(4)
Co(2)—O(5)	2.067(4)	Co(2)—N(2)	2.293(4)
O(3)—Co(1)—N(1)	77.9(2)	O(1)—Co(1)—N(1)	76.9(2)
O(9)—Co(1)—N(3)	76.3(2)	O(11)—Co(1)—N(3)	78.2(2)
O(15)—Co(2)—N(4)	78.4(2)	O(13)—Co(2)—N(4)	76.9(2)
O(7)—Co(2)—N(2)	78.8(2)	O(5)—Co(2)—N(2)	76.4(2)
N(1)—Co(1)—N(3)	118.6(2)	N(2)—Co(2)—N(4)	117.4(2)
O(11)—Co(1)—O(3)	158.3(2)	O(9)—Co(1)—N(1)	161.1(2)
O(1)—Co(1)—N(3)	161.2(2)	O(5)—Co(2)—N(4)	162.8(2)
O(7)—Co(2)—O(15)	157.2(2)	O(13)—Co(2)—N(2)	162.9(2)
<b>(b) in the <i>p</i>-PhDTA ligand</b>			
C(21)—N(3)	1.479(6)	C(22)—C(21)	1.526(7)
O(9)—C(22)	1.270(6)	C(23)—N(3)	1.478(6)
N(3)—C(15)	1.462(7)	C(24)—C(23)	1.527(7)
O(11)—C(24)	1.267(6)	N(1)—C(9)	1.470(6)
N(1)—C(7)	1.486(7)	C(7)—C(8)	1.512(8)
C(8)—O(1)	1.274(7)	C(9)—C(10)	1.530(8)
C(10)—O(3)	1.272(6)	N(4)—C(25)	1.478(7)
N(4)—C(27)	1.483(6)	C(27)—C(28)	1.503(8)
C(28)—O(14)	1.244(7)	C(28)—O(13)	1.267(7)
C(26)—O(16)	1.236(6)	C(26)—O(15)	1.263(7)
C(11)—N(2)	1.488(6)	N(2)—C(4)	1.458(7)
N(2)—C(13)	1.468(7)	C(13)—C(14)	1.523(7)
C(14)—O(8)	1.247(6)	C(14)—O(7)	1.261(6)
C(1)—N(1)	1.450(6)	C(22)—O(10)	1.237(6)
O(12)—C(24)	1.237(6)	C(18)—N(4)	1.452(7)
C(8)—O(2)	1.241(7)	C(10)—O(4)	1.228(7)
C(21)—N(3)—Co(1)	101.5(3)	C(23)—N(3)—Co(1)	100.0(3)
N(3)—C(21)—C(22)	112.7(4)	O(9)—C(22)—C(21)	116.7(5)
C(22)—O(9)—Co(1)	117.6(3)	N(3)—C(23)—C(24)	111.3(4)
O(11)—C(24)—C(23)	116.3(5)	C(24)—O(11)—Co(1)	118.8(3)
C(7)—N(1)—Co(1)	100.8(3)	N(1)—C(7)—C(8)	111.2(5)
O(1)—C(8)—C(7)	118.0(5)	C(8)—O(1)—Co(1)	116.4(3)
C(9)—N(1)—Co(1)	101.0(3)	N(1)—C(9)—C(10)	111.2(4)
O(3)—C(10)—C(9)	115.6(5)	C(10)—O(3)—Co(1)	119.0(4)
C(25)—N(4)—Co(2)	100.8(3)	N(4)—C(25)—C(26)	111.7(4)
O(15)—C(26)—C(25)	116.3(5)	C(26)—O(15)—Co(2)	118.9(4)
C(27)—N(4)—Co(2)	100.5(3)	N(4)—C(27)—C(28)	111.1(4)
O(13)—C(28)—C(27)	118.6(5)	C(28)—O(13)—Co(2)	116.3(3)
C(11)—N(2)—Co(2)	101.9(3)	N(2)—C(11)—C(12)	112.8(4)
O(5)—C(12)—C(11)	117.0(5)	C(12)—O(5)—Co(2)	117.8(3)
C(13)—N(2)—Co(2)	99.9(3)	N(2)—C(13)—C(14)	111.6(4)
O(7)—C(14)—C(13)	116.3(5)	C(14)—O(7)—Co(2)	118.1(3)
<b>(c) Coordination sphere of the sodium</b>			
Na(1)—O(6 <sup>W</sup> )	2.291(5)	Na(1)—O(8 <sup>W</sup> )	2.319(5)
Na(3)—O(3 <sup>W</sup> )	2.307(5)	Na(4)—O(5 <sup>W</sup> )	2.544(6)
Na(1)—O(12)	2.273(5)	Na(2)—O(14)	2.298(5)
Na(3)—O(8)	2.304(4)	Na(2)—O(8 <sup>W</sup> )	2.520(6)
Na(2)—O(6 <sup>W</sup> <sup>i</sup> )	2.640(6)	Na(3)—O(5 <sup>W</sup> )	2.312(5)
Na(4)—O(3 <sup>W</sup> <sup>i</sup> )	2.602(6)	Na(1)—O(16 <sup>ii</sup> )	2.310(4)
Na(4)—O(10 <sup>iii</sup> )	2.421(5)	Na(2)—O(6 <sup>i</sup> )	2.432(5)
Na(4)—O(5 <sup>iii</sup> )	2.302(4)	Na(2)—O(9 <sup>iv</sup> )	2.324(5)
Na(4)—O(2 <sup>iv</sup> )	2.300(5)	Na(1)—O(6 <sup>v</sup> )	2.383(4)
Na(3)—O(10 <sup>vi</sup> )	2.379(4)	Na(3)—O(4 <sup>vii</sup> )	2.265(5)

Atoms with roman numeral superscripts are related to those of the asymmetric unit by the transformations: (i)  $-x+1, -y, -z$ ; (ii)  $-x+1/2, y+1/2, -z$ ; (iii)  $-x+1, -y-1/2, z-1/2$ ; (iv)  $-x+1/2, y-1/2, -z$ ; (v)  $x, y+1/2, -z+1/2$ ; (vi)  $-x+1/2, y, z+1/2$ ; (vii)  $x+1/2, -y, -z+1/2$ .

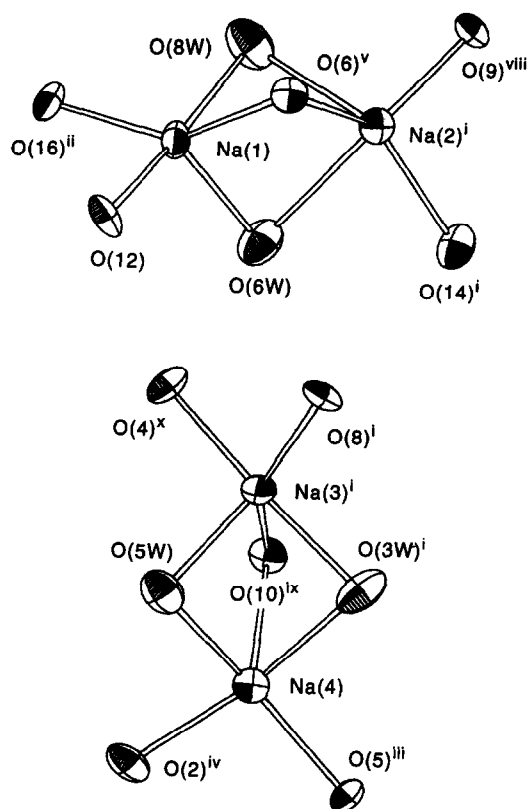


Fig. 10. Coordination geometry of the sodium atoms in  $\text{Na}_4[\text{Co}_2(p\text{-PhDTA})_2] \cdot 8\text{H}_2\text{O}$  with the atomic numbering schemes shown in Table 5 and the transformations: (viii)  $x + 1/2, -y + 1/2, z$ ; (ix)  $x + 1/2, -y, -z - 1/2$ ; (x)  $-x + 1/2, y, z - 1/2$ . Ellipsoids are plotted at the 50% probability level.

same metal atoms. In the  $[\text{Co}_2(p\text{-PhDTA})_2]^{4-}$  dimer complex (Fig. 9), the two triangular faces formed by the three donor atoms (ONO) of each iminodiacetate group make dihedral angles of  $30.1(1)^\circ$  for Co(1) and  $27.6(1)^\circ$  for Co(2), similar to the value for the  $[\text{Co}_2(m\text{-PhDTA})_2]^{4-}$ ,  $26.9(1)^\circ$  [9], maintaining the cobalt atoms 1.22 and 1.24 Å [Co(1)] and 1.22 and 1.25 Å [Co(2)], apart from these planes. There are similar values for  $[\text{Co}_2(m\text{-PhDTA})_2]^{4-}$ , 1.293(1) Å. These peculiar interplanar angles are larger than the values observed for monomer complexes  $[\text{Co}(o\text{-PhDTA})]^{2-}$  [36] and  $[\text{Co}(4\text{-Cl-}o\text{-PhDTA})]^{2-}$  [37], and this is fundamentally the reason for the distortion observed for the idealized octahedral cobalt environment. We have calculated [38,39] and compared the degree of distortion of  $\text{CoN}_2\text{O}_4$  octahedra for the dimer complexes  $[\text{Co}_2(p\text{-PhDTA})_2]^{4-}$  and  $[\text{Co}_2(m\text{-PhDTA})_2]^{4-}$  [9] (Table 6). It is observed that the octahedra in  $p\text{-PhDTA}$  dimer complex are slightly more distorted than in the  $m\text{-PhDTA}$  dimer complex, as expected.

The Co—O bond distances (Table 5) [average 2.043(4) Å for Co(1) and 2.045(4) Å for Co(2)] are similar to those of the  $[\text{Co}_2(m\text{-PhDTA})_2]^{4-}$  complex [9] [average 2.049(2) Å]. These bond distances com-

Table 6. Degree of distortion of  $\text{CoN}_2\text{O}_4$  octahedra for **1**,  $[\text{Co}_2(p\text{-PhDTA})_2]^{4-}$ , and **2**,  $[\text{Co}_2(m\text{-PhDTA})_2]^{4-}$

Distortion ( $\times 10^3$ )	<b>1</b> , Co(1)	<b>1</b> , Co(2)	<b>2</b> , Co
$\Delta l$	3.26	3.13	2.91
$\Delta e$	12.3	11.4	11.1
$\Delta \alpha$	12.1	11.4	9.74

The octahedral distortion has been calculated using equations (1)–(3):

$$\Delta l = 1/6 \sum [(R_i - R)/R]^2 \quad (1)$$

$$\Delta e = 1/12 \sum [(D_i - D)/D]^2 \quad (2)$$

$$\Delta \alpha = 1/3 \sum [(\alpha_i - 180)/180]^2, \quad (3)$$

where  $R_i$  = an individual Co—O or Co—N distance,  $R$  = the mean Co—O or Co—N distance,  $D_i$  = an individual O—O or O—N distance,  $D$  = the mean O—O or O—N distance and  $\alpha_i$  = an individual O—Co—O or O—Co—N angle.

pare well with the separations previously reported in polyaminocarboxylate transition-metal complexes (range 1.89–2.08 Å) [36,37,40,41]. However, the Co—N bond distances observed in the dimer complexes  $[\text{Co}_2(p\text{-PhDTA})_2]^{4-}$  (Table 5) [average 2.300(4) Å for Co(1) and 2.295(4) Å for Co(2)] and  $[\text{Co}_2(m\text{-PhDTA})_2]^{4-}$  [average 2.289(2) Å] [9] are markedly longer than those determined for the related monomer complexes  $[\text{Co}(\text{EDTA})]^{2-}$  (2.160 Å) [36],  $[\text{Co}(o\text{-PhDTA})]^{2-}$  (2.184 Å) [36] and  $[\text{Co}(4\text{-Cl-}o\text{-PhDTA})]^{2-}$  (2.198 Å) [37].

The planes of the “glycine” chelate rings M—O—C—C—N—M have been calculated and classified according to Hoard’s proposal [42]. Rings Co(1)—N(3)—C(21)—C(22)—O(9), Co(1)—N(1)—C(7)—C(8)—O(1), Co(2)—N(4)—C(27)—C(28)—O(13) and Co(2)—N(2)—C(11)—C(12)—O(5) are of the type G (more nearly parallel to the NMN plane), and rings Co(1)—N(3)—C(23)—C(24)—O(11), Co(1)—N(1)—C(9)—C(10)—O(3), Co(2)—N(4)—C(25)—C(26)—O(15) and Co(2)—N(2)—C(13)—C(14)—O(7) are of type R (more nearly perpendicular to the NMN plane).

The four crystallographically independent sodium ions are five-coordinated involving interactions with three oxygen atoms from carboxylate groups and two waters of crystallization (Fig. 10). According to the angles and distances, the coordination of the Na(2) and Na(4) ions may be described as two distorted square-based pyramids with O(6<sup>v</sup>) and O(10<sup>ix</sup>) in the apical positions, respectively, and the planes O(6W)—O(14<sup>i</sup>)—O(9<sup>viii</sup>)—O(6<sup>v</sup>) and O(5W)—O(2<sup>iv</sup>)—O(5<sup>iii</sup>)—O(3W<sup>i</sup>) forming the bases. The atoms Na(2<sup>i</sup>) and Na(4) are out of the basal planes by 0.59 Å. The sodium ions Na(1) and Na(3) are coordinated in a more distorted, nearly trigonal bipyramid configuration. The coordination spheres in each of the

two metal containing ions [Na(1)—Na(2') and Na(3')—Na(4)] have a face in common. Although this type of environment for Na<sup>+</sup> is not very common, a similar situation has been observed in the complexes Na<sub>4</sub>[Co<sub>2</sub>(*m*-PhDTA)<sub>2</sub>·10H<sub>2</sub>O and Na<sub>4</sub>[Ni<sub>2</sub>(2,6-PyDTA)<sub>2</sub>·8H<sub>2</sub>O [9] (2,6-PyDTA = pyridine-2,6-diamine-*N,N',N',N'*-tetraacetic acid). In these complexes one oxygen atom from a carboxylate group bridges two Na<sup>+</sup> ions.

*Supplementary material.* Z(pH) curves simulating for a three-component system the formation of monomer and polymer complexes (Figs S1 a–d), Z(pH) curves for the Cu<sup>II</sup>-ligand system (*I* = 0.1, Fig. S2), species distribution diagrams for the Ni<sup>II</sup>-ligand (ligand:metal ratios 2:1 and 1:1) and Co<sup>II</sup>-ligand systems (ratios 1:1 and 1:2, Figs S3 and S4), and Zn<sup>II</sup>-ligand and Cd<sup>II</sup>-ligand systems (Figs S5 and S6), with figure captions are included. Tables of atomic coordinates and equivalent isotropic displacement parameters, complete bond lengths and angles, least-squares mean planes, anisotropic displacement parameters, hydrogen coordinates and isotropic displacement parameters, and observed and calculated structure factors, are also included (46 pages). Ordering information is given on any current masthead page.

*Acknowledgements*—We wish to thank the Education Council of the Canary Islands Government (Grants No 27/08.03.90 and 93/032, 1994) and the Spanish Ministry of Education and Science (DGICYT, Grants No PB89-0401 and APC 94-0031) for financial support, and the Computer Center of the Faculty of Sciences (UCV) for computer time at Unisys A10 and Silicon Graphics Challenge Computer Systems. One of us (FB) is also indebted to the Consejo de Desarrollo Científico y Humanístico (CDCH) of the Central University of Venezuela (UCV) and to the University of La Laguna for the benefit of Studies Assistantship in the Department of Inorganic Chemistry of the University of La Laguna (ULL) during 1994. JMA acknowledges the UPV-EHU project 169.310-EB057/93.

## REFERENCES

- Uhlig, E. and Herrmann, D., *Z. Anorg. Allg. Chem.*, 1968, **360**, 158.
- Ruiz-Pérez, C., Rodríguez, M. L., Rodríguez-Romero, F. V., Mederos, A., Gili, P. and Martín-Zarza, P., *Acta Cryst.*, 1990, **C46**, 1405.
- Mederos, A., Rodríguez González, A. and Rodríguez Ríos, B., *An. Quim.*, 1970, **66**, 531.
- Rodríguez Ríos, B. and Mederos, A., *An. Quim.*, 1969, **65B**, 649.
- Uhlig, E. and Herrmann, D., *Z. Anorg. Allg. Chem.*, 1968, **359**, 135.
- Mederos, A., Felipe, J. M., Brito, F. and Bazdikian, K., *J. Coord. Chem.*, 1986, **14**, 285.
- Bruto, F., Mederos, A., Gili, P., Domínguez, S. and Martín-Zarza, P., *J. Coord. Chem.*, 1988, **17**, 311.
- Bruto, F., Mederos, A., Gili, P., Guerra, R., Domínguez, S. and Hernández-Padilla, M., *J. Coord. Chem.*, 1989, **20**, 169.

- Mederos, A., Gili, P., Domínguez, S., Benitez, A., Palacios, M. S., Hernández-Padilla, M., Martín-Zarza, P., Rodríguez, M. L., Ruiz-Pérez, C., Lahoz, F. J., Oro, L. A., Brito, F., Arrieta, J. M., Vlasi, M. and Germain, G., *J. Chem. Soc., Dalton Trans.*, 1990, 1477.
- Domínguez, S., Rancel, A., Herrera, J. V., Mederos, A. and Brito, F., *J. Coord. Chem.*, 1992, **25**, 271.
- Domínguez, S., Mederos, A., Gili, P., Rancel, A., Rivero, A. E., Brito, F., Lloret, F., Rodríguez, M. L., Brito, I., Solans, X. and Ruiz-Pérez, C., *Inorg. Chim. Acta*, in press.
- Blasius, E. and Olbricht, G., *Z. Analyt. Chem.*, 1956, **151**, 81.
- Fontanelli, M. and Micheloni, M., "A Modern Computer Controlled Potentiometric Titration System for Equilibrium Studies", I Spanish-Italian Congress on Thermodynamics of Metal Complexes, p. 41. Peñíscola; Servicio de Publicaciones, Diputación de Castellón, Spain, 1990.
- Biederman, G. and Sillén, L. G., *Arkiv. Kemi.*, 1953, **5**, 425.
- Bruto, F. and Gonçalves, J. M., Project no. 51.78.31-S1-1228, CONICIT, Caracas, 1981.
- Ingri, N. and Sillén, L. G., *Arkiv. Kemi.*, 1964, **23**, 97.
- Bruto, F. and Ingri, N., *An. Fis. Quim.*, 1960, **56B**, 165.
- Bruto, F., personal communication, 1994.
- Gans, P., Sabatini, A. and Vacca, A., *J. Chem. Soc., Dalton Trans.*, 1985, 1195.
- Sillén, L. G., *Master Variables and Activity Scales. Adv. in Chem., Ser. (Am. Chem. Soc.)*, 1967, **67**, 45.
- Mederos, A., Rodríguez González, A. and Rodríguez Ríos, B., *An. Quim.*, 1973, **69**, 601.
- Mederos, A., Manrique, F. G., Herrera, J. V., Alvarez-Romero, M. and Felipe, J. M., *An. Quim.*, 1986, **82B**, 133.
- Orvig, C., *J. Chem. Educ.*, 1985, **62**, 84.
- Jones, P., *Chem. Brit.*, 1981, **17**, 222.
- Sheldrick, G. M., *Acta Cryst.*, 1990, **A46**, 467.
- Sheldrick, G. M., *SHELXL93. Program for the Refinement of Crystal Structures*. University of Göttingen, Germany, 1993.
- International Tables for Crystallography*, Vol. C. Kluwer Academic Publishers, Dordrecht, 1992.
- Bruto, F., Gili, P., Mederos, A., Domínguez, S. and Rivero, A. E., *J. Coord. Chem.*, 1990, **21**, 29.
- Baer Jr, Ch. F. and Mesmer, R. E., *The Hydrolysis of Cations*. Wiley, New York, 1976.
- Sillén, L. G., *Belief and Facts about Polyions*. Proc. of Symposium on Coordination Chemistry, Tihany, Hungary, 1964.
- Ingri, N. and Brito, F., *Acta Chem. Scand.*, 1959, **13**, 1971.
- Meloun, M., Havel, J. and Hogfeldt, E., *Computation of Solution Equilibria*. Ellis Horwood Limited, New York, 1988.
- Beck, M. T. and Nagypál, I., *Chemistry of Complex Equilibria*. Ellis Horwood Limited, New York, 1990.

34. Uhlig, E. and Herrmann, D., *Z. Chem.*, 1964, **4**, 463.
35. Johnson, C. K., ORTEP, Report ORNL-3794, Oak Ridge National Laboratory, Oak Ridge, TN, 1971.
36. McCandlish, E. F. K., Michael, T. K., Neal, J. A., Lingafelter, E. C. and Rose, N. J., *Inorg. Chem.*, 1978, **17**, 1383.
37. Hernández-Padilla, M., Domínguez, S., Gili, P., Mederos, A. and Ruiz-Pérez, C., *Polyhedron*, 1992, **11**, 1965.
38. Martín-Zarza, P., Arrieta, J. M., Muñoz-Roca, M. C. and Gili, P., *J. Chem. Soc., Dalton Trans.*, 1993, 1551.
39. Roman, P., Gutiérrez-Zorrilla, J. M., Martínez-Ripoll, M. and García Blanco, S., *Polyhedron*, 1986, **5**, 1799.
40. Azuma, S., Nakasuka, N. and Tanaka, M., *Acta Cryst.*, 1986, **C42**, 673.
41. Nakasuka, N., Azuma, S. and Tanaka, M., *Acta Cryst.*, 1986, **C42**, 1485.
42. Weakliem, H. E. and Hoard, J. L., *J. Am. Chem. Soc.*, 1959, **81**, 549.